Chinese Journal of Natural Medicines

Dimeric sesquiterpenoids with anti-inflammatory activities from *Inula britannica*

Juan Zhang, Jiankun Yan, Hongjun Dong, Rui Zhang, Jing Chang, Yanli Feng, Xinrong Xu, Wei Li, Feng Qiu, Chengpeng Sun

Citation: Juan Zhang, Jiankun Yan, Hongjun Dong, Rui Zhang, Jing Chang, Yanli Feng, Xinrong Xu, Wei Li, Feng Qiu, Chengpeng Sun, Dimeric sesquiterpenoids with anti-inflammatory activities from *Inula britannica*, Chinese Journal of Natural Medicines, 2025, 23(8), 961-971. doi: 10.1016/S1875-5364(25)60931-9.

View online: https://doi.org/10.1016/S1875-5364(25)60931-9

Chinese Journal of Natural Medicines 23 (2025) 961-971

Contents lists available at ScienceDirect

Chinese Journal of Natural Medicines

journal homepage: www.cjnmcpu.com/

Original article

Dimeric sesquiterpenoids with anti-inflammatory activities from *Inula britannica*

Juan Zhang[a,Δ], Jiankun Yan[b,Δ], Hongjun Dong[c,Δ], Rui Zhang[a], Jing Chang[a], Yanli Feng[a], Xinrong Xu[a], Wei Li[d], Feng Qiu[a,*], Chengpeng Sun[a,*]

[a] *School of Chinese Materia Medica, Tianjin Key Laboratory of Therapeutic Substance of Traditional Chinese Medicine, Tianjin University of Traditional Chinese Medicine, Tianjin 301617, China*

[b] *School of Pharmacy, Hebei University of Chinese Medicine, Shijiazhuang 050200, China*

[c] *Second Affiliated Hospital, Dalian Medical University, Dalian 116044, China*

[d] *Faculty of Pharmaceutical Sciences, Toho University, Chiba 274-8510, Japan*

ARTICLE INFO

Article history:
Received 2 July 2024
Revised 23 September 2024
Accepted 9 December 2024
Available online 20 August 2025

Keywords:
Inula britannica
Sesquiterpenoid dimers
Anti-inflammatory effects
Mechanism
Keap1-Nrf2

ABSTRACT

In continuation of research aimed at identifying anti-inflammatory agents from natural sesquiterpenoids, an activity-guided fractionation approach utilizing lipopolysaccharide (LPS)-mediated RAW264.7 cells was employed to investigate chemical constituents from *Inula Britannica* (*I. britannica*). Seven novel sesquiterpenoid dimers inulabritanoids A–G (**1**–**7**) and two novel sesquiterpenoid monomers inulabritanoids H (**8**) and I (**9**) were isolated from *I. britannica* together with eighteen known compounds (**10**–**27**). The structural elucidation was accomplished through comprehensive analysis of 1D and 2D nuclear magnetic resonance (NMR), high-resolution mass spectrometry (HR-MS), and electronic circular dichroism (ECD) spectra, complemented by quantum chemical calculations. Compounds **1**, **2**, **12**, **16**, **19**, and **26** demonstrated inhibitory effects on NO production, with IC_{50} values of 3.65, 5.48, 3.29, 6.91, 3.12, and 5.67 μmol·L^{-1}, respectively. Mechanistic studies revealed that compound **1** inhibited IκB kinase β (IKKβ) phosphorylation, thereby blocking nuclear factor κB (NF-κB) nuclear translocation, and activated the kelch-like ECH-associated protein 1 (Keap1)/nuclear factor erythroid 2-related factor 2 (Nrf2) signal pathway, leading to decreased expression of NADPH oxidase 2 (NOX-2), inducible nitric oxide synthase (iNOS), tumor necrosis factor α (TNF-α), interleukin-6 (IL-6), monocyte chemotactic protein-1 (MCP-1), IL-1β, and IL-1α and increased expression of NAD(P)H: quinone oxidoreductase 1 (NQO-1) and heme oxygenase-1 (HO-1), thus exhibiting anti-inflammatory effects *in vitro*. These results indicate that dimeric sesquiterpenoids may serve as promising candidates for anti-inflammatory drug development.

1. Introduction

Inula Britannica (*I. britannica*), a member of the genus *Inula* in the Asteraceae family, is widely distributed throughout Asia and Europe, including Korea, Japan, China, and Russia [1, 2]. According to the *Chinese Pharmacopoeia*, flowers of *I. britannica* and *I. japonica* constitute the traditional Chinese medicine Inulae Fols, known as "Xuan Fu Hua" in Chinese [1, 3]. *I. britannica* exhibits therapeutic properties, including expectorant, cough suppressant, and anti-bacterial effects [4]. Modern medical practice frequently incorporates *I. britannica* into classic formulations for treating gastric distention and hardness, particularly in preparations such as Xuanfu-Daizhe Decoction and Huatan-Jiangqi Prescription. Pharmacological studies have demonstrated that *I. britannica* possesses diverse biological functions, including anti-inflammatory [5], anti-oxidant [6], anti-bacterial [7], anti-cancer [8, 9], and pulmonary protective effects [10]. The extract of Inulae Fols, for instance, ameliorates lipopolysaccharide (LPS)- and bleomycin-mediated acute lung injury and pulmonary fibrosis by regulating soluble epoxide hydrolase (sEH) and kelch-like ECH-associated protein 1 (Keap1) [11-13]. Thus, *I. britannica* warrants extensive research attention.

Recent comprehensive investigations of the genus *Inula* have resulted in the isolation and identification of sesquiterpenoids, diterpenoids, and flavonoids, including inubritanolides A–D [14, 15], britanicafanins A–E [2], spiroalanfurantones A–D [16], and inulajaponicolide A [17]. Notably, sesquiterpenoids demonstrate significant biological activities due to their distinctive *α,β*-unsaturated lactone, encompassing anti-inflammatory [18] and neuroprotective effects [15, 19], as well as sEH inhibition [2, 20]. Furthermore, our research group has demonstrated that wedelolactone isolated from *I. britannica* mitigates acute lung injury by targeting sEH through suppression of inflammation and oxidation stress [21]. These findings indicate the importance of further investigating the chemical

* Corresponding author.
E-mail addresses: fengqiu20070118@163.com (F. Qiu); suncp146@163.com (C. Sun)
Δ These authors contributed equally to this work.

https://doi.org/10.1016/S1875-5364(25)60931-9

constituents of *I. britannica*.

In continuation of our research on biological natural products, the extract of *I. britannica* yielded 27 sesquiterpenoids, guided by inhibitory activity toward NO production [22]. These compounds include 7 new dimers inulabritanoids A–G (**1**–**7**), 2 new monomers inulabritanoids H (**8**) and I (**9**), and 18 known analogues (**10**–**27**) (Fig. 1). Structure elucidation was accomplished through 1D and 2D nuclear magnetic resonance (NMR), high-resolution mass spectrometry (HR-MS), and electronic circular dichroism (ECD) spectra analysis, complemented by quantum chemical calculations. The isolated compounds underwent evaluation for anti-inflammatory effects, and the mechanisms underlying their anti-inflammatory action were investigated. This research sought to implement a strategy for isolating active constituents while expanding the therapeutic applications of *I. britannica.*

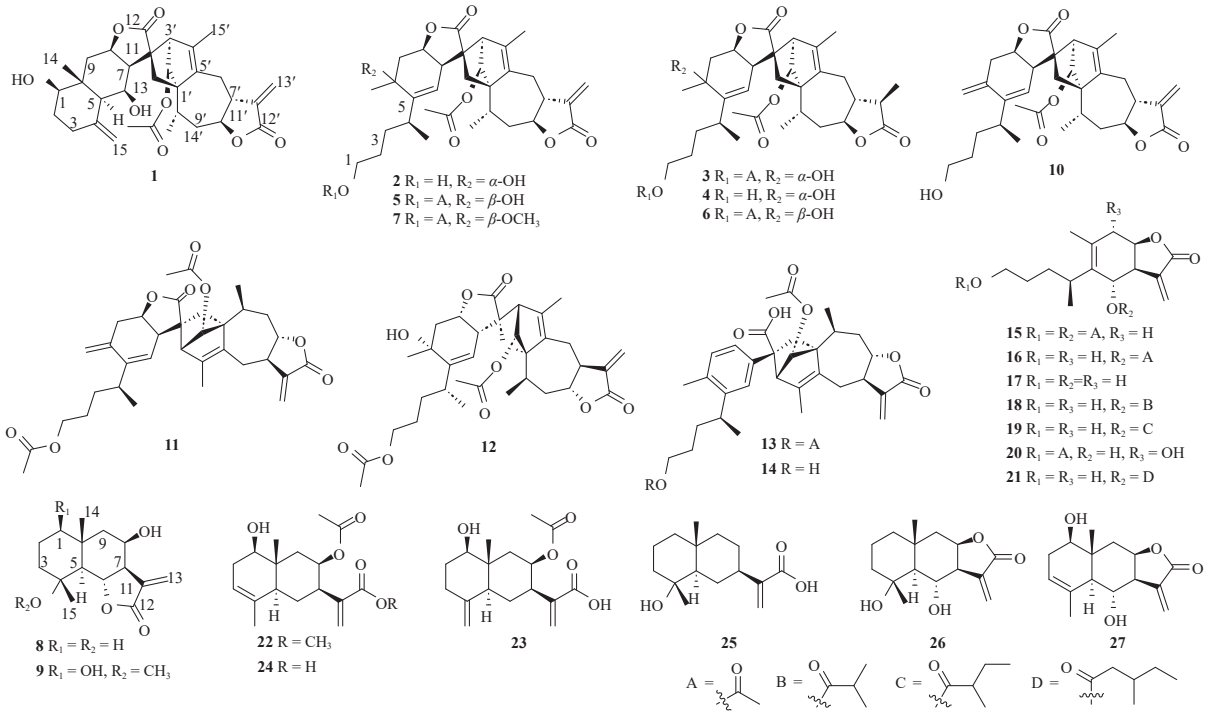

Fig. 1 Structures of compounds **1**–**27** isolated from *I. britannica.*

2. Results and discussion

2.1. Structural characterization

An activity-guided fractionation strategy using LPS-stimulated RAW264.7 macrophages was employed to isolate and identify anti-inflammatory constituents of *I. britannica*. Fractions E4 and E5 exhibited significant anti-inflammatory effects and were subsequently selected for detailed separation. 27 Sesquiterpenoids were isolated from *I. britannica*, comprising 7 new dimers inulabritanoids A–G (**1**–**7**), 2 new monomers inulabritanoids H (**8**) and I (**9**), and 18 known analogues inulanolide C (**10**) [23], inulanolide F (**11**) [24], japonicone D (**12**) [25], inulanolide E (**13**) [26], inulanolide D (**14**) [23], 1,6-*O*,*O*-diacetylbritannilactone (**15**) [27], 6*α*-acetoxy-1-hydroxy-4*αH*-1,10-secoeudesma-5(10),11(13)-dien-8*β*,12-olide (**16**) [28], 1,6*α*-dihydroxyeriolanolide (**17**) [27], 6*α*-isobutyryloxy-1-hydroxy-4*αH*-1,10-secoeudesma-5(10),11(13)-dien-8*β*,12-olide (**18**) [28], 6*α*-(2-methybutyryloxy)-1-hydroxy-4*αH*-1,10-secoeudesma-5(10),11(13)-dien-8*β*,12-olide (**19**) [28], 1,10-secoeudesmanolide (**20**) [27], 6*α*-(3-methylvaleryloxy)-1-hydroxy-4*αH*-1,10-secoeudesma-5(10),11(13)-dien-8*β*,12-olide (**21**) [28], 1*β*-hydroxy-8*β*-acetoxyisocostic acid methyl ester (**22**) [29], inujaponin B (**23**) [30], inujaponin C (**24**) [30], ilicic acid (**25**) [31], 4*α*,6*α*-dihydroxyeudesman-8*β*,12-olide (**26**) [32], and desacetyl-*α*-cyclopyrethrosin (**27**) [33].

Inulabritanoid A (**1**) exhibited a molecular formula of $C_{32}H_{40}O_8$ based on its positive HR-MS data at *m/z* 553.2798 [M + H]$^+$ (Calcd. for $C_{32}H_{41}O_8^+$, 553.2796) and ^{13}C NMR data. The ^{1}H NMR spectrum (Table 1) revealed signals corresponding to three methyl groups [δ_H 1.71 (3H, s), 0.99 (3H, s), and 0.95 (3H, d, *J* = 6.2 Hz)], an acetyl group [δ_H 2.06 (3H, s)], an *α*,*β*-unsaturated lactone group [δ_H 5.96 (1H, d, *J* = 2.5 Hz), 5.68 (1H, d, *J* = 2.5 Hz), and 4.18 (1H, s)], and one exocyclic double bond [δ_H 4.86 (1H, br s) and 4.68 (1H, br s)]. Furthermore, four protons attached to oxygenated carbons appeared at δ_H 4.67 (1H, m), 4.52 (1H, m), 4.17 (1H, br s), and 3.32 (1H, dd, *J* = 12.0, 3.2 Hz) in the low field of its ^{1}H NMR spectrum. The ^{13}C NMR spectrum indicated 32 carbon resonances, including two ester carboxyl carbons at δ_C 180.6 and 169.7, three pairs of double bonds at δ_C 144.6, 140.6, 136.3, 134.8, 118.0, and 108.0, five oxygenated carbons at δ_C 80.8, 80.3, 76.7, 71.4, and 67.1, suggesting that **1** was a dimeric sesquiterpenoid in conjunction with its ^{1}H NMR data [25]. Comparative analysis of ^{13}C NMR data between **1** and japonicone A from *I. japonica* revealed notable differences in carbon resonances [25]. The chemical shifts at C-4 and C-15 in japonicone A were observed at δ_C 38.2 and 23.0, respectively, while these shifts moved downfield to δ_C 144.6 and 118.1 in **1**. Conversely, chemical shifts at C-5 and C-6 in japonicone A [25], originally at δ_C 149.5 and 118.1, shifted upfield to δ_C 54.1 and 67.1 in **1**, respectively. These spectral changes indicated the presence of a $\Delta^{4(15)}$ double bond and a hydroxy group at C-6 in **1**. Heteronuclear multiple bond correlation (HMBC) from H-15a/H-15b to C-3/C-5 and H-7 to C-5/C-6 supported this deduction (Fig. 2). The relative configuration of 1 was established through nuclear Overhauser effect spectroscopy (NOESY) correlations from CH_3-14 to OH-1/OH-6, H-1 with H-5/H-8, H-5 to H-6/H-7, H-7 to H-8/H-3′, CH_3-14′ to H-2′/H-8′, and H-7′ to H-13a (Fig. 3), demonstrating *β*-orientations of OH-1, OH-6, H-7′, and CH_3-14, *α*-orientations of H-2′, H-7, H-8, H-8′, and CH_3-14′, and (11*R**)-configuration. The absolute configuration of

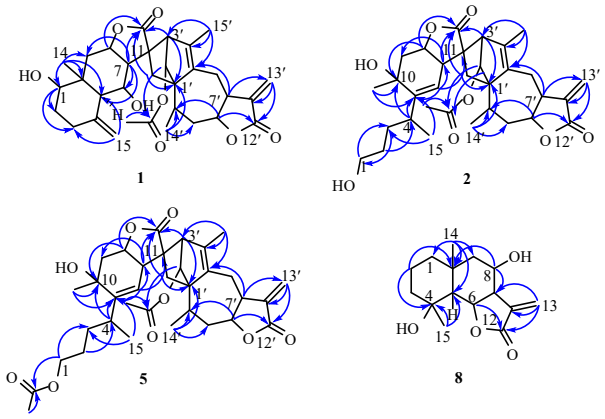

Fig. 2 Key HMBC correlations of compounds **1**, **2**, **5**, and **8**.

1 was determined through ECD spectrum calculation at the B3LYP/6-311G(d) level. The calculated ECD spectrum of 1*R*,5*S*,6*S*,7*S*,8*R*,10*R*,11*R*,1′*S*,2′*S*,3′*R*,7′*R*,8′*S*,10′*S*-**1** matched its experimental spectrum (Fig. 4), confirming the (1*R*,5*S*,6*S*,7*S*,8*R*,10*R*,11*R*,1′*S*,2′*S*,3′*R*,7′*R*,8′*S*,10′*S*)-configuration of **1**, consistent with the X-ray crystal result of inubritanolide A isolated from *I. britannica* and its biosynthetic pathway [15].

Inulabritanoid B (**2**) exhibited a molecular formula of $C_{32}H_{42}O_8$ based on its HR-MS spectrum (*m/z* 555.2961 [M + H]$^+$, Calcd. for $C_{32}H_{43}O_8^+$, 555.2952). The ^{1}H NMR data (Table 1) of **2** indicated the presence of three olefinic signals [δ_H 6.07 (1H, d, *J* = 3.2 Hz), 5.77 (1H, d, *J* = 3.2 Hz), and 5.30 (1H, d, *J* = 2.5 Hz)], five oxygenated protons [δ_H 4.95 (1H, m), 4.48 (1H, br s), 4.30 (1H, m), 3.34 (1H, m), and 3.32 (1H, m)], an acetyl group [δ_H 2.02 (3H, s)], and three methyl groups [δ_H 1.59 (3H, s), 1.09 (3H, s), and 1.04 (3H, d, *J* = 6.7 Hz)]. The ^{13}C NMR data of **2** revealed two ester carboxyl carbons (δ_C 178.7 and 169.5), six olefinic carbons (δ_C 151.6, 139.8, 136.8, 133.0, 119.2, and 115.0), one acetyl moiety (δ_C 169.5 and 20.8), and five oxygenated carbons (δ_C 82.0, 80.9, 74.6, 67.6, and 61.0). The NMR data were comparable to those of japonicone D (**12**) [25]. Notably, the C-1 chemical shift value (δ_C 64.3) in **12** was shielded to δ_C 61.0 in **2**, and signals of an acetyl moiety (δ_C 171.0 and 20.9; δ_H 2.08) in **12** were absent in **2** [25], indicating that **2** was a C-1 deacetyl derivative of **12**. This was confirmed by HMBC cross-peaks from H-1a/H-1b to C-3 and H-3a to C-1 (Fig. 2). The NOESY spectrum correlations from H-7 to OH-10/H-8/H-3′, CH_3-14′ to H-2′/H-8′, and H-7′ to H-13a (Fig. 3) established a *β*-orientation of H-7′, *α*-orientations of H-2′, H-7, H-8, H-8′, OH-10, and CH_3-14′, and a (11*R**)-configuration. The (4*S*,7*R*,8*R*,10*R*,11*S*,1′*S*,2′*S*,3′*R*,7′*R*,8′*S*,10′*S*)-configuration was determined based on the similarity between experimental and calculated ECD spectra of **2** (Fig. 4) and its biosynthetic pathway [15].

Analysis of HR-MS data for inulabritanoid C (**3**) (*m/z* 599.3218 [M + H]$^+$, Calcd. for $C_{34}H_{47}O_9^+$, 599.3215) and inulabritanoid F (**6**) (*m/z* 599.3218 [M + H]$^+$, Calcd. for $C_{34}H_{47}O_9^+$, 599.3215) established their molecular formula as $C_{34}H_{46}O_9$. Their comparable ^{1}H and ^{13}C NMR data (Tables 1 and 2) indicated that **3** and **6** shared an identical plane with the dimeric sesquiterpenoid skeleton analogous to **2**, consistent with their molecular formula. A comprehensive comparison of their NMR data revealed distinct configurations at C-10, evidenced by ^{13}C shift values of C-5, C-9, and C-10 being shielded from δ_C 151.0, 40.7, and 67.5 in **3** to δ_C 148.9, 39.6, and 66.5 in **6**, respectively, while δ_C 115.4 of C-6 in **3** was deshielded to δ_C 116.6 in **6**. These variations indicated an *α*-orientation of OH-10 in **3** and a *β*-orientation of OH-10 in **6**, confirmed by NOESY correlations of H-7 with OH-10 in **3** and H-7 with CH_3-14 in **6**. The experimental spectra of **3** and **6** exhibited similar positive Cotton effects at 207 and 232 nm, and their 7*R*,8*R*,10*R*,11*S*,1′*S*,2′*S*,3′*R*,7′*R*,8′*S*,10′*S*,11′*R* ECD spectra calculated at the B3LYP/6-311G(d) level corresponded with their experimental results (Fig. 4), confirming their 4*S*,7*R*,8*R*,10*R*,11*S*,1′*S*,2′*S*,3′*R*,7′*R*,8′*S*,10′*S*,11′*R*-configurations in conjunction with the X-ray crystal result of inubritanolide A isolated from *I. britannica* [15].

Inulabritanoid D (**4**) exhibited a molecular formula of $C_{32}H_{44}O_8$ based on its HR-MS data (*m/z* 555.2968 [M − H]$^-$, Calcd. for $C_{32}H_{43}O_8^-$, 555.2963). Comparison of NMR data of **4** and **2** indicated structural similarity except for the $\Delta^{11'(13')}$ double bond, evidenced by the upfield shift of C-11′ and C-13′ from δ_C 139.8 and 119.2 in **2** to δ_C 42.6 and 9.5 in **4**, respectively, and the downfield shift of C-12′ from δ_C 169.5 in **2** to δ_C 179.0 in **4**. The HMBC between CH_3-13′ and C-7′/C-11′/C-12′ indicated the reduction of the $\Delta^{11'(13')}$ double bond in **4**. The *α*-configuration of OH-10 was determined through the correlation of CH_3-13′ with H-7′ in the NOESY spectrum of **4**. The ECD spectrum of **4** displayed positive Cotton effects at 205 and 231 nm, corresponding to its calculated ECD (Fig. 4), establishing a (4*S*,7*R*,8*R*,10*R*,11*S*,1′*S*,2′*S*,3′*R*,7′*R*,8′*S*,10′*S*,11′*R*)-configuration in accordance with its biosynthetic pathway [15].

Inulabritanoid E (**5**) was determined to have a molecular formula of $C_{34}H_{44}O_9$. Analysis of ^{1}H and ^{13}C NMR data between **5** and **2** revealed variations at C-1 and C-10. The HMBC of H-1a/OAc-CH_3 with OAc-CO in **5** confirmed the acetyl moiety position at C-1 (Fig. 2). Additionally, C-5 (δ_C 151.6 in **2**) and C-10 (δ_C 67.6 in **2**) chemical shifts were shielded to δ_C 148.8 and 66.5 in **5**, while the C-5 (δ_C 115.0 in **2**) chemical shift was deshielded to δ_C 116.6 in **5**, indicating a *β*-orientation of OH-10, supported by the NOESY correlation of H-8 with CH_3-14 (Fig. 3). The calculated ECD spectra of 7*R*,8*R*,10*S*,11*S*,1′*S*,2′*S*,3′*R*,7′*R*,8′*S*,10′*S*-**5** matched its experimental spectrum (Fig. 4), confirming its 4*R*,7*R*,8*R*,10*S*,11*S*,1′*S*,2′*S*,3′*R*,7′*R*,8′*S*,10′*S*-configuration in conjunction with the X-ray crystal result of inubritanolide A isolated form *I. britannica* [15].

1D and 2D NMR and HR-MS (611.3223 [M + H]$^+$, Calcd. for $C_{35}H_{47}O_9^+$, 611.3215) data indicated that inulabritanoid G (**7**) was a sesquiterpenoid dimer with a molecular formula of $C_{35}H_{46}O_9$. The ^{1}H and ^{13}C NMR data (Table 3) of **7** exhibited close similarity to those of **5**, with the notable distinction that **7** contained an additional methoxy moiety (δ_C 49.3 and δ_H 3.06). The downfield shift of C-10 from δ_C 66.5 in **5** to δ_C 73.1 in **7** indicated their structural difference. The HMBC of OCH_3-10 with C-10 and the NOESY correlation of H-7 with CH_3-14 established that **7** was a 10*β*-*O*-methylated derivative of **5**. The (4*S*,7*R*,8*R*,10*S*,11*S*,1′*S*,2′*S*,3′*R*,7′*R*,8′*S*,10′*S*)-configuration of **7** was determined through comparison of its experimental and calculated ECD spectra (Fig. 4) and its biosynthesis background [15].

Inulabritanoid H (**8**) exhibited a molecular formula of $C_{15}H_{22}O_4$ as determined by its HR-MS spectrum. Comparison of ^{1}H and ^{13}C NMR data (Table 4) between **8** and 8*β*-hydroxy-*β*-cyclocostunolide revealed that chemical shift values of C-4 and C-15 were shielded from δ_C 144.1 and 109.2 in 8*β*-hydroxy-*β*-cyclocostunolide to δ_C 72.1 and 24.5 in **8** [34], indicating that **8** was a hy-

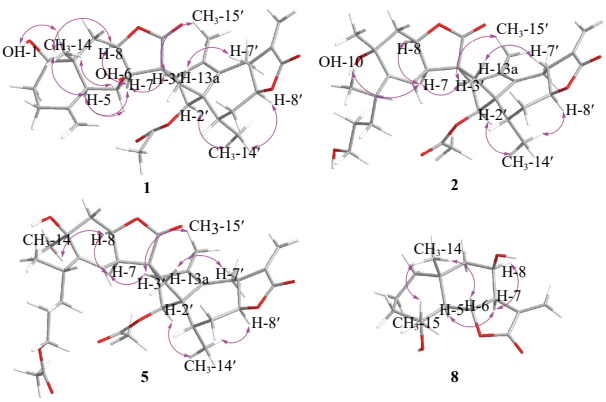

Fig. 3 Key NOESY correlations of compounds **1**, **2**, **5**, and **8**.

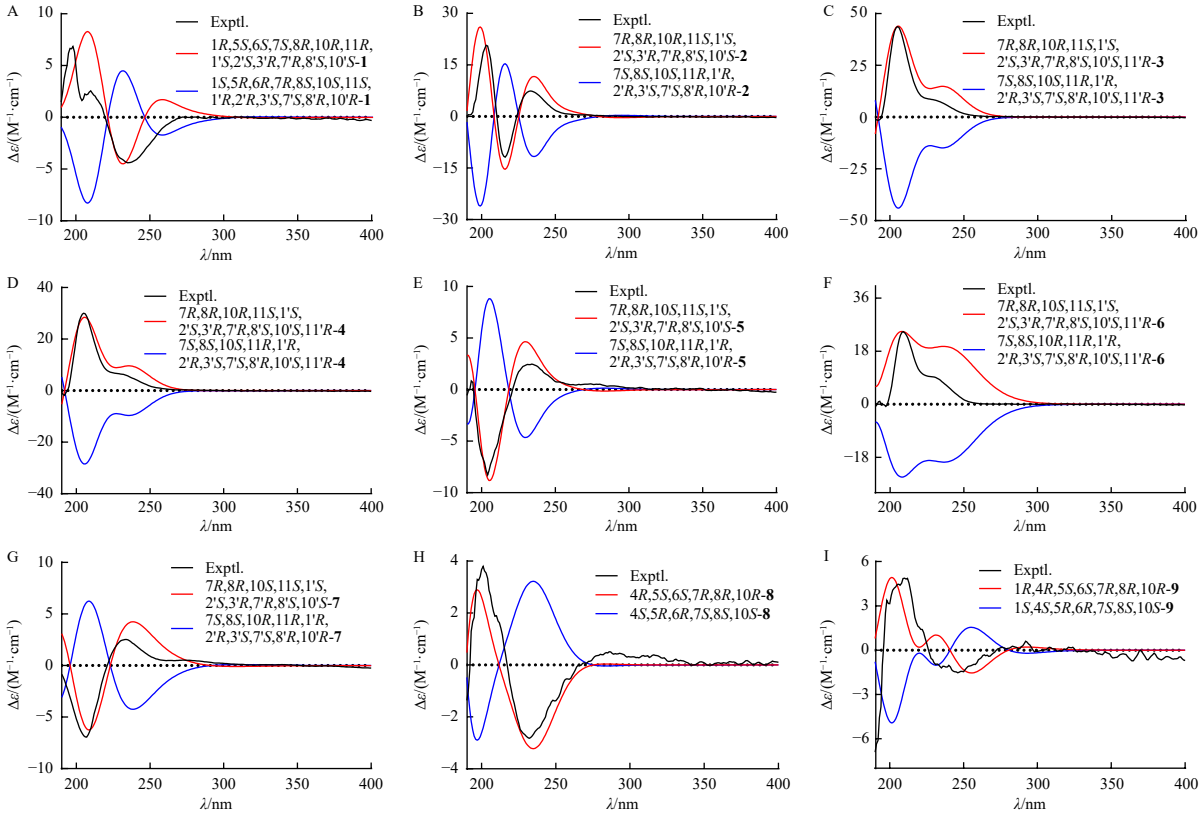

Fig. 4 Experimental and calculated ECD spectra of compounds **1–9** (A–I) at the B3LYP/6-311G(d) level.

drated derivative of 8*β*-hydroxy-*β*-cyclocostunolide. HMBC from CH_3-15 to C-4 and H-5 to C-4/15 (Fig. 2) confirmed the location of a hydroxy moiety at C-10 in **8**. In its NOESY spectrum, correlations between CH_3-14 with H-6/CH_3-15 and H-7 with H-5/H-8 (Fig. 3) established *β*-orientations of H-6, OH-8, CH_3-14, and CH_3-15, and *α*-orientations of H-5 and H-7. As illustrated in Fig. 4, the ECD spectrum of (4*R*,5*S*,6*S*,7*R*,8*R*,10*R*)-**8** calculated at the B3LYP/6-311G(d) level matched its experimental ECD spectrum, confirming a (4*R*,5*S*,6*S*,7*R*,8*R*,10*R*)-configuration.

Analysis of NMR data of inulabritanoid I (**9**) and **8** revealed the location of a hydroxy moiety at C-1 and the methylation of a hydroxy moiety at C-4, evidenced by the downfield shift of C-1 and C-4 from δ_C 41.2 and 72.1 in **8** to δ_C 77.1 and 74.8 in **9**, respectively, and the presence of a methoxy moiety (δ_C 47.3 and δ_H 3.03) in **9**. The HMBC from CH_3-14 to C-1 and OCH_3-4 to C-4 supported this structural assignment. Its NOESY and experimental and calculated ECD spectra confirmed the (1*R*,4*R*,5*S*,6*S*,7*R*,8*R*,10*R*)-configuration of **9**.

2.2. Anti-inflammatory effects

The isolated compounds were evaluated for their anti-inflammatory effects on NO production (Table 5). Compounds **1**, **2**, **12**, **16**, **19**, and **26** exhibited significant inhibition of NO release with IC_{50} values of 3.65, 5.48, 3.29, 6.91, 3.12, and 5.67 μmol·L^{-1}, respectively, in LPS-mediated RAW264.7 cells. Compounds **5**, **7**, **11**, **13**, **17**, and **20** demonstrated moderate anti-inflammatory effects with IC_{50} values ranging from 10.02 to 19.58 μmol·L^{-1}. Comparison of IC_{50} values between **10** with **11** and **14** with **13** indicated that OAc-1 influenced anti-inflammatory effects in dimeric sesquiterpenoids, as IC_{50} values of **10** and **14** exceeded 40 μmol·L^{-1}, while those of **11** and **13** were 10.02 and 11.14 μmol·L^{-1}, respectively. The *α*,*β*-unsaturated lactone demonstrated a crucial role in anti-inflammatory effects for sesquiterpenoid dimers. For 1,10-secoeudestanes, deacetylation of C-1 in **15** enhanced its anti-inflammatory effects (IC_{50}, 24.77 μmol·L^{-1} for **15**; IC_{50}, 6.91 μmol·L^{-1} for **16**).

2.3. Compound *1* inhibited the inflammatory response in vitro

To evaluate the anti-inflammatory potential of compound **1**, we assessed its effects on LPS-induced inflammatory responses in RAW264.7 macrophages. Following LPS stimulation, treatment with compound **1** inhibited NO production (Fig. 5A). Additionally, compound **1** significantly reduced the secretion of tumor necrosis factor α (TNF-α) and interleukin-6 (IL-6) in LPS-treated RAW264.7 cells, with a particularly pronounced reduction in IL-6 (Figs. 5B and 5C). Furthermore, the effects of compound **1** on intracellular cytokines and chemokines, monocyte chemotactic protein-1 (MCP-1), IL-6, IL-1β, and IL-1α, were examined. The results showed that compound **1** also suppressed the LPS-stimulated increase in the mRNA levels of *MCP-1*, *IL-6*, *IL-1β*, and *IL-1α* stimulated by LPS (Fig. 5D).

2.4. Compound *1* regulated the IκB kinase β (IKKβ)/nuclear factor κB (NF-κB) -mediated cytokine storm

The NF-κB pathway is a pivotal regulator of the inflammatory response [21,35-39]. In the classical inflammatory signaling pathway, IKKβ phosphorylation triggers the ubiquitylation and degradation of IκBα to activate the NF-κB pathway [40], subsequently promoting the release of IL-1β, TNF-α, and IL-6. These cytokines can subsequently activate the NF-κB pathway, establishing a positive feedback loop that enhances inflammatory response [41]. Therefore, this study investigated whether the effects of compound **1** were attributable to its inhibitory activity on the IKKβ/NF-κB pathway. Compound **1** demonstrated inhibition of key NF-κB proteins [including inducible nitric oxide synthase (iNOS), cyclooxygenase-2 (COX-2), phosphorylated (p)-p65, and p-IKKβ] (Figs. 6A and 6B). This inhibitory activity was further confirmed through immunofluorescence experiments (Fig. 6C), which clearly demonstrated the reduction in iNOS expression by

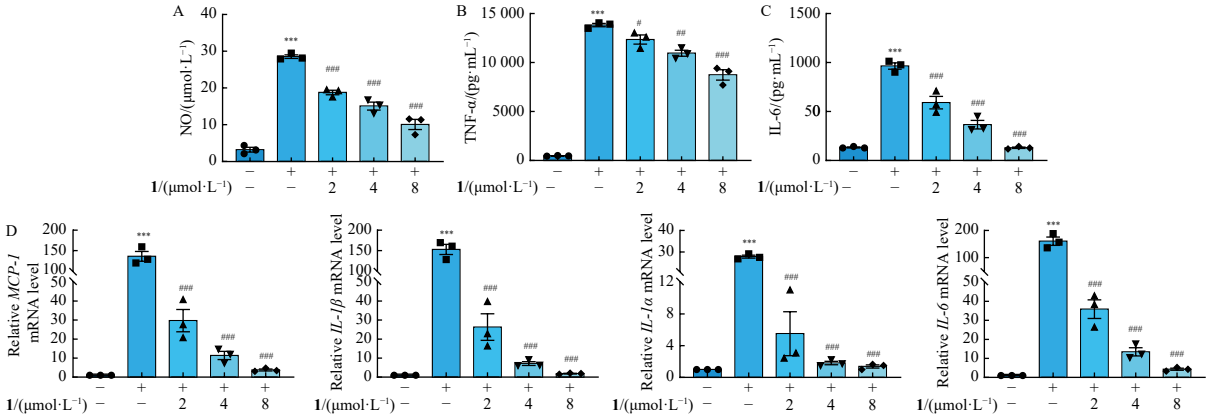

Fig. 5 Compound **1** inhibited the release of NO (A), TNF-α (B), and IL-6 (C) in RAW264.7 cells stimulated by LPS; (D) Compound **1** reduced the mRNA expressions of *MCP-1*, *IL-1β*, *IL-1α*, and *IL-6* in LPS-stimulated RAW264.7 cells. Data were expressed as the mean ± SEM (n = 3). $^{***}P < 0.001$ *vs* Control; $^{\#}P < 0.05$, $^{\#\#}P < 0.01$, $^{\#\#\#}P < 0.001$ *vs* LPS.

compound **1**. As demonstrated above, compound **1** exhibited its anti-inflammatory effects *via* inhibition of the IKKβ/NF-κB-mediated cytokine storm.

*2.5. Compound **1** regulated cellular oxidation levels through the nuclear factor erythroid 2-related factor 2 (Nrf2) signaling pathway*

During inflammation, activated macrophages release numerous pro-inflammatory mediators, which subsequently stimulate the production of ROS, thereby amplifying the inflammatory response [42]. To examine the potential regulatory effects of compound **1** on oxidative stress levels, we examined its influence on key gene and protein expressions within the Nrf2 signaling pathway. Quantitative polymerase chain reaction (PCR) analysis, as shown in Fig. 7A, confirmed that compound **1** attenuated the upregulation of NADPH oxidase 2 (*NOX-2*) and restored the expression of NAD(P)H: quinone oxidoreductase 1 (*NQO-1*). Furthermore, compound **1** significantly upregulated the mRNA and protein expressions of heme oxygenase-1 (HO-1) and Nrf2 (Figs. 7B and 7C), while reducing Keap1 expression. These findings demonstrated the regulatory capacity of compound **1** on the Nrf2 signaling pathway.

3. Conclusion

In summary, this investigation examined chemical constituents from *I. britannica*, yielding seven new sesquiterpenoid dimers inulabritanoids A–G (**1**–**7**) and two new sesquiterpenoid monomers inulabritanoids H (**8**) and I (**9**), along with eighteen known analogues (**10**–**27**). Compounds **1**, **2**, **12**, **16**, **19**, and **26** exhibited potent anti-inflammatory effects with IC_{50} values of 3.12–6.91 μmol·L^{-1}. Subsequent mechanism studies revealed that compound **1** inactivated the IKKβ-NF-κB pathway and activated the Keap1-Nrf2 pathway, demonstrating its anti-inflammatory properties. These results indicate that sesquiterpenoids represent promising candidates for anti-inflammatory drug development.

4. Experimental

4.1. General experimental procedures

NMR spectra were obtained using a Bruker AV-600 spectrometer (Bruker, Bremerhaven, Germany), with peak signals of DMSO-d_6 and $CDCl_3$ serving as references. HR-MS spectra of new compounds were analyzed using a Waters Xevo G2S QTOF high-resolution mass spectrometer (Waters Corp., Milford, MA, USA). MeOH, EtOH, EtOAc, and CH_2Cl_2 were obtained from Concord Technology (Tianjin, China). Silica gel (300–400 mesh; Qingdao Haiyang Chemical Co., Ltd., Qingdao, China) and ODS RP-C_{18} (40–63 μm, FuJi, Aichi, Japan) were employed for column chromatography (CC) separation. A Waters ACQUITY Arc system (California, USA) with an Innoval ODS-2 (5 μm, 4.6 mm × 250 mm, Tianjin, China) column was utilized for high-performance liquid chromatography (HPLC) analysis. Preparative HPLC was performed using a SEP LC-51 system [Separation (Beijing) Technology Co., Ltd., Beijing, China] with a MWD UV detector and a YMC-Pack ODS-A column (5 μm, 250 mm × 20 mm, YMC Co., Ltd., Kyoto, Japan).

4.2. Plant material

The whole plant of *I. britannica* was collected from Liaoning Province, China, in 2018, and identified by Prof. Jingming Jia (Shenyang Pharmaceutical University, Shenyang, China). The voucher specimen (IB201806) was deposited in Tianjin University of Traditional Chinese Medicine.

4.3. Extraction and isolation

The plants of *I. britannica* (8.6 kg) were extracted using 95% EtOH (100 L × 2 h × 2 times) and 75% EtOH (100 L × 2 h × 2 times), successively. The 95% and 75% EtOH extracts were combined and concentrated at 45 °C *in vacuo*. The extracts were suspended in H_2O (5 L) and extracted with equivalent EtOAc three times. The resulting 315.8 g of extract underwent silica gel CC elution with a gradient mixture of CH_2Cl_2 and MeOH (from 100∶1 to 1∶1), yielding eleven fractions E1–E11. Fraction E4 was separated through silica gel CC eluted with petroleum ether–acetone (from 50∶1 to 1∶1), producing seven subfractions E41–E47. E43 underwent purification by polyamide (MeOH–H_2O, from 1∶1 to 9∶1) and ODS CC (10%–100% MeOH), where subfraction E4312 was isolated *via* preparative HPLC (50%–80% MeCN) to yield compound **15** (3.3 mg), **16** (2.0 mg), **19** (5.0 mg), and **20** (3.0 mg). E44 was purified through polyamide CC (MeOH–H_2O, from 1∶1 to 9∶1), yielding seven subfractions E441–E447. Compounds **5** (4.2 mg), **6** (3.2 mg), **7** (3.2 mg), **8** (5.6 mg), **9** (2.0 mg), and **18** (2.8 mg) were obtained from fraction E441 through Sephadex LH-20 CC (MeOH) and preparative HPLC (50%–80% MeCN). Fraction E447 was separated *via* ODS CC (10%–90% MeOH), yielding twelve subfractions E4471–E44712, and subfractions E4479 and E44712 were isolated by preparative HPLC (50% CH_3CN for E4479; 60% CH_3CN for E44712) to obtain compounds **11** (3.2 mg) and **13** (3.6 mg). Fraction E45 underwent purification through a Sephadex LH-20 column with MeOH elution, yielding fourteen subfractions E451–E4514. Compounds **14** (2.0 mg), **21** (2.3 mg), **22** (5.0 mg), **25** (59.5 mg), and **26** (3.4 mg) were isol-

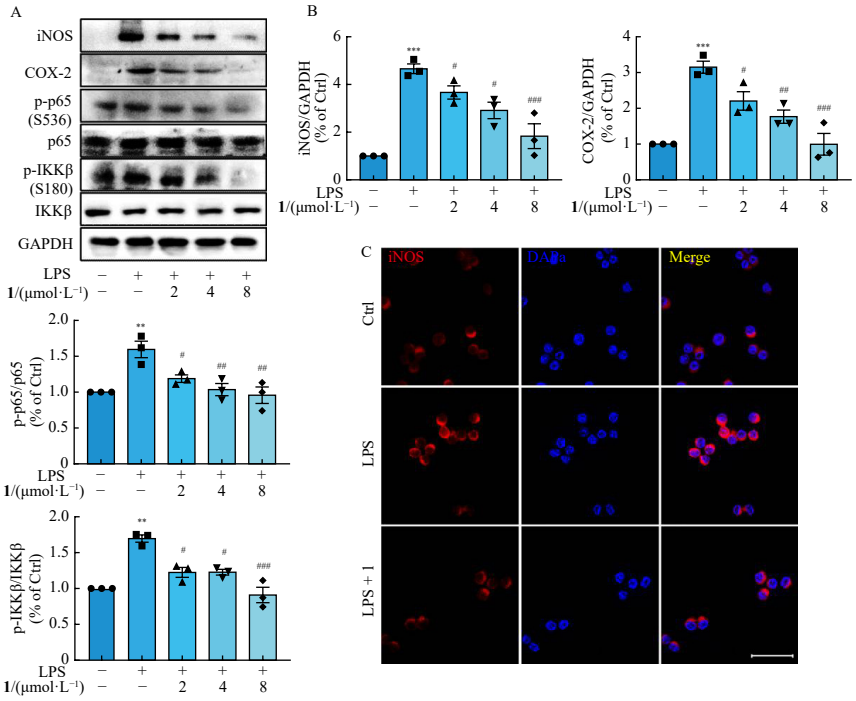

Fig. 6 (A) Compound **1** downregulated expressions of iNOS, COX-2, p-p65, and p-IKKβ; (B) Quantitative results of iNOS, COX-2, p-p65, and p-IKKβ; (C) Representative plots of iNOS immunofluorescence. Data were expressed as the mean ± SEM (n = 3). $^{**}P < 0.01$, $^{***}P < 0.001$ *vs* Control; $^{\#}P < 0.05$, $^{\#\#}P < 0.01$, $^{\#\#\#}P < 0.001$ *vs* LPS.

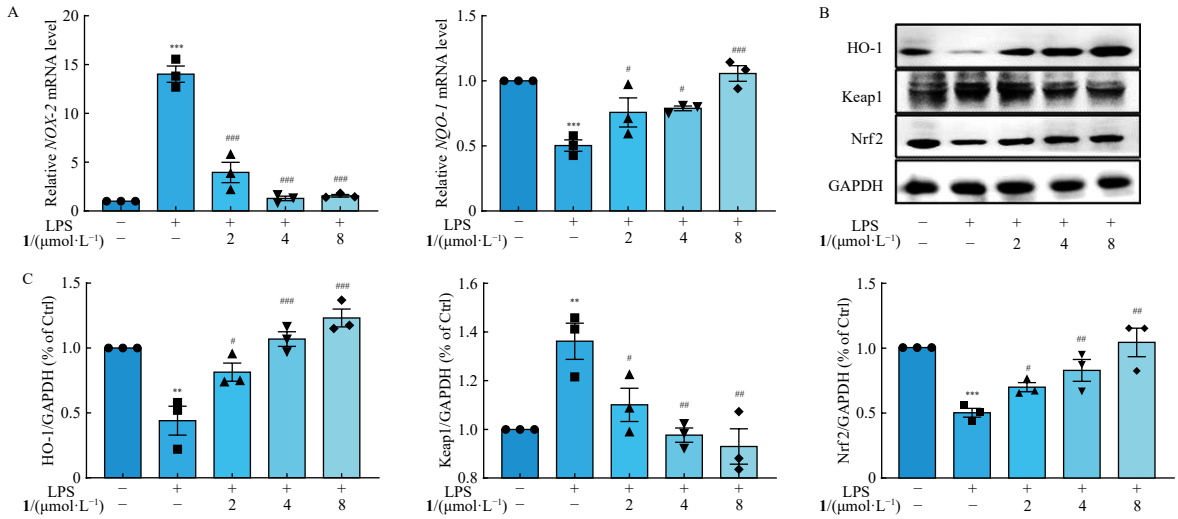

Fig. 7 (A) Compound **1** downregulated mRNA expression of *NOX-2* and upregulated mRNA expression of *NQO-1*; (B) Compound **1** regulated protein expressions of HO-1, Keap1, and Nrf2; (C) Quantitative results of HO-1, Keap1, and Nrf2. Data were expressed as the mean ± SEM (n = 3). $^{**}P < 0.01$, $^{***}P < 0.001$ *vs* Control; $^{\#}P < 0.05$, $^{\#\#}P < 0.01$, $^{\#\#\#}P < 0.001$ *vs* LPS.

ated from subfractions E452, E453, and E455 *via* preparative HPLC (30%–60% CH_3CN), respectively. Fraction E456 purification through ODS CC (10%–90% MeOH) and preparative HPLC (50%–70% CH_3CN) yielded compounds **3** (7.7 mg), **4** (2.2 mg), **10** (2.2 mg), **12** (10.9 mg), **23** (4.9 mg), and **24** (6.0 mg). Fraction E458 underwent separation by ODS CC with gradient MeOH and H_2O elution (from 1∶9 to 9∶1), followed by preparative HPLC (60%–75% MeOH) to obtain compounds **1** (5.0 mg) and **2** (4.0 mg). Fraction E4514 was isolated through preparative HPLC with 35% CH_3CN elution to yield compound **17** (28.8 mg). Finally, compound **27** (5.0 mg) was obtained from fraction E5 through silica gel CC (CH_2Cl_2–acetone, from 100∶1 to 1∶1), ODS CC (10%–90% MeOH), and preparative HPLC (40% CH_3CN).

Inulabritanoid A (**1**): colorless powder; $[\alpha]_D^{25}$ +43 (*c* 0.1, MeOH); ECD (MeOH) nm (Δε) 198 (+6.84), 235 (−4.39); ^{1}H and ^{13}C NMR data (Table 1); HR-MS *m/z* 553.2798 $[M + H]^+$ (Calcd. for $C_{32}H_{41}O_8^+$, 553.2796).

Inulabritanoid B (**2**): colorless powder; $[\alpha]_D^{25}$ +44 (*c* 0.1, MeOH); ECD (MeOH) nm (Δε) 203 (+20.71), 216 (−11.84), 234 (+7.37); ^{1}H and ^{13}C NMR data, (Table 1); HR-MS *m/z* 555.2961 $[M + H]^+$ (Calcd. for $C_{32}H_{43}O_8^+$, 555.2952).

Inulabritanoid C (**3**): colorless powder; $[\alpha]_D^{25}$ +45 (*c* 0.1, MeOH); ECD (MeOH) nm (Δε) 207 (+43.70), 232 (+7.89); ^{1}H and ^{13}C NMR data (Table 1); HR-MS *m/z* 599.3218 $[M + H]^+$ (Calcd. for $C_{34}H_{47}O_9^+$, 599.3215).

Inulabritanoid D (**4**): colorless powder; $[\alpha]_D^{25}$ +44 (*c* 0.1, MeOH); ECD (MeOH) nm (Δε) 205 (+30.02), 231 (+6.38); ^{1}H and ^{13}C NMR data (Table 2); HR-MS *m/z* 555.2968 $[M - H]^-$ (Calcd. for $C_{32}H_{43}O_8^-$, 555.2963).

Inulabritanoid E (**5**): colorless powder; $[\alpha]_D^{25}$ +42 (*c* 0.1, MeOH); ECD (MeOH) nm (Δε) 204 (−8.28), 234 (+2.47); ^{1}H and ^{13}C NMR data (Table 2); HR-MS *m/z* 595.2892 $[M - H]^-$ (Calcd. for

Table 1 ^{1}H (600 MHz) and ^{13}C NMR (150 MHz) data for compounds. **1–3** in DMSO-d_6

No.	1		2		3	
	δ_C	δ_H (J in Hz)	δ_C	δ_H (J in Hz)	δ_C	δ_H (J in Hz)
1	76.7	3.32, dd (12.0, 3.2)	61.0	3.34, m	63.9	3.98, m
				3.32, m		3.89, m
2	30.6	1.63, m	31.0	1.29, m	26.5	1.40, m
		1.46, m		1.25, m		1.36, m
3	33.4	2.19, m	34.2	1.35, m	33.4	1.35, m
		2.05, m		1.31, m		1.31, m
4	144.6		31.7	2.40, m	31.7	2.44, m
5	54.1	2.14, m	151.6		151.0	
6	67.1	4.67, m	115.0	5.30, d (2.5)	115.4	5.30, d (2.4)
7	51.3	2.07, m	41.4	2.90, m	41.3	2.91, m
8	71.4	4.52, m	74.6	4.95, m	74.5	4.94, m
9	44.5	2.12, m	40.7	2.26, dd (14.6, 2.9)	40.7	2.26, m
		1.39, m		1.85, m		1.85, dd (14.5, 1.9)
10	41.5		67.6		67.5	
11	55.3		56.2		56.3	
12	180.6		178.7		178.5	
13	31.1	3.36, d (11.7)	35.9	1.95, d (12.2)	35.7	1.94, d (12.1)
		1.26, d (11.7)		1.72, d (12.2)		1.72, d (12.1)
14	14.3	0.99, s	28.8	1.09, s	28.8	1.10, s
15	108.0	4.86, br s	23.6	1.04, d (6.7)	23.9	1.05, d (6.7)
		4.68, br s				
1′	67.3		61.9		61.7	
2′	80.3	4.17, br s	80.9	4.48, br s	80.8	4.47, br s
3′	47.4	2.56, br s	55.1	2.92, m	55.0	2.90, br s
4′	134.8		133.0		132.2	
5′	136.3		136.8		137.3	
6′	25.6	3.09, br d (15.3)	25.1	3.01, br d (15.8)	23.6	2.62, m
		2.01, m		2.11, m		2.07, m
7′	45.4	2.78, br t (9.8)	44.7	2.69, t (10.3)	39.8	2.61, m
8′	80.8	4.18, m	82.0	4.30, m	81.1	4.51, td (11.5, 3.7)
9′	35.7	2.25, m	35.4	2.21, td (12.9, 3.0)	35.5	2.20, dt (12.4, 3.7)
		1.44, m		1.87, m		1.78, td (12.4, 2.4)
10′	26.0	2.23, m	29.1	2.05, m	29.1	2.02, m
11′	140.6		139.8		42.4	2.26, m
12′	169.7		169.5		179.0	
13′	118.0	5.96, d (2.5)	119.2	6.04, d (3.2)	9.5	1.13, d (7.8)
		5.68, d (2.5)		5.77, d (3.2)		
14′	17.5	0.95, d (6.2)	16.6	0.96, s (7.2)	16.6	0.97, d (7.2)
15′	13.2	1.71, s	14.0	1.59, s	13.8	1.52, s
OH-1		4.52, d (4.0)		4.29, t (4.5)		
OH-6		4.56, d (1.5)				
OH-10				4.52, s		4.54, s
OAc-1					170.1	
					20.6	1.93, s
OAc-2′	170.2		169.5		169.6	
	20.8	2.06, s	20.8	2.02, s	20.8	2.02, s

Table 2 ^{1}H (600 MHz) and ^{13}C NMR (150 MHz) data of compounds **4**–**6** in DMSO-d_6.

No.	**4**		**5**		**6**	
	δ_C	δ_H (J in Hz)	δ_C	δ_H (J in Hz)	δ_C	δ_H (J in Hz)
1	61.0	3.33, t (6.0)	64.0	3.96, m	64.0	3.96, m
				3.83, m		3.84, m
2	30.9	1.28, m	26.1	1.39, m	26.1	1.40, m
		1.25, m		1.37, m		1.38, m
3	34.2	1.32, m	33.7	1.37, m	33.8	1.37, m
		1.31, m		1.32, m		1.32, m
4	31.6	2.4, m	31.7	2.40, m	31.7	2.40, m
5	151.7		148.8		148.9	
6	114.9	5.30, d (2.8)	116.6	5.40, d (1.7)	116.6	5.40, d (2.0)
7	41.4	2.90, m	41.5	2.90, dd (5.0, 2.4)	41.5	2.90, dd (5.1, 2.5)
8	74.6	4.94, m	74.2	4.92, m	74.2	4.91, m
9	40.7	2.26, dd (14.6, 3.2)	39.7	2.23, m	39.6	2.23, m
		1.85, dd (14.6, 1.8)		1.84, dd (14.5, 2.4)		1.85, dd (14.5, 1.9)
10	67.5		66.5		66.5	
11	56.1		57.0		56.9	
12	178.7		178.3		178.2	
13	35.9	1.94, d (12.1)	35.7	2.00, d (12.1)	35.8	1.99, d (12.1)
		1.71, d (12.1)		1.74, d (12.1)		1.74, d (12.1)
14	28.8	1.09, s	28.2	1.21, s	28.2	1.21, s
15	23.5	1.03, d (6.7)	23.0	1.03, d (6.7)	22.9	1.03, d (6.7)
1′	61.6		62.0		61.7	
2′	80.9	4.46, br s	80.8	4.48, br s	80.8	4.46, br s
3′	55.1	2.89, m	55.1	2.94, br s	55.1	2.92, d (1.3)
4′	132.2		133.1		132.3	
5′	137.3		136.7		137.3	
6′	23.9	2.63, m	25.1	3.01, br d (15.5)	23.9	2.63, m
		2.07, m		2.11, m		2.07, m
7′	39.7	2.63, m	44.6	2.73, t (10.1)	39.4	2.63, m
8′	81.1	4.50, dd (11.4, 3.8)	82.0	4.30, td (11.1, 3.1)	81.1	4.51, dd (11.4, 3.6)
9′	35.6	2.21, t (13.9)	35.3	2.22, m	35.6	2.21, m
		1.75, m		1.94, m		1.75, d (12.1)
10′	29.1	2.04, m	29.1	2.06, m	29.1	1.99, d (12.2)
11′	42.6	2.22, m	139.9		42.4	2.26, m
12'	179.0		169.5		179.8	
13′	9.5	1.13, d (7.7)	119.1	6.05, d (3.2)	9.5	1.13, d (7.7)
				5.77, d (3.2)		
14′	16.6	0.97, d (7.2)	16.6	0.97, d (7.2)	16.6	0.97, d (7.2)
15′	13.9	1.52, s	14.0	1.60, s	13.9	1.53, s
OH-10		4.50, s		3.56, s		3.56, s
OA_C-1			170.1		170.1	
			20.6	1.88, s	20.9	1.92, s
OA_C-2′	169.6		169.7		116.9	
	20.8	2.02, s	20.9	2.03, s	20.7	2.02, s

Table 3 ^{1}H (600 MHz) and ^{13}C NMR (150 MHz) data for compound **7** in DMSO-d_6.

No.	δ_C	δ_H (J in Hz)	No.	δ_C	δ_H (J in Hz)
1	63.4	3.97, m	1′	61.6	
		3.87, m	2′	80.4	4.48, br s
2	25.8	1.45, m	3′	54.4	2.95, br s
		1.38, m	4′	132.6	
3	34.1	1.35, m	5′	136.5	
		1.29, m	6′	25.9	1.35, m
4	30.4	2.38, m			1.15, m
5	148.3		7′	44.2	2.72, m
6	118.9	5.51, d (2.4)	8′	81.6	4.30, td (11.2, 3.6)
7	40.8	2.95, m	9′	35.0	2.22, m
8	74.0	5.00, m			1.95, m
9	39.4	2.61, m	10′	28.7	2.07, m
		2.35, m	11′	139.5	
10	73.1		12′	169.2	
11	56.1		13′	118.7	6.05, d (3.2)
12	178.0				5.77, d (3.2)
13	35.1	2.00, d (12.1)	14′	16.2	0.97, d (7.2)
		1.73, d (12.1)	15′	13.6	1.60, s
14	25.9	1.15, s	OAc-2′	169.3	
15	20.9	1.04, d (6.7)		20.5	2.04, s
OAc-1	169.8		OCH_3-10	49.3	3.06, s
	20.2	1.90, s			

$C_{34}H_{43}O_9^-$, 595.2913).

Inulabritanoid F (**6**): colorless powder; $[\alpha]_D^{25}$ +45 (*c* 0.1, MeOH); ECD (MeOH) nm (Δε) 207 (+24.41), 232 (+8.79); ^{1}H and ^{13}C NMR data (Table 2); HR-MS *m/z* 599.3209 $[M + H]^+$ (Calcd. for $C_{34}H_{47}O_9^+$, 599.3215).

Inulabritanoid G (**7**): colorless powder; $[\alpha]_D^{25}$ +37 (*c* 0.1, MeOH); ECD (MeOH) nm (Δε) 208 (−6.71), 233 (+2.53); ^{1}H and ^{13}C NMR data (Table 3); HR-MS *m/z* 611.3223 $[M + H]^+$ (Calcd. for $C_{35}H_{47}O_9^+$, 611.3215).

Inulabritanoid H (**8**): colorless powder; $[\alpha]_D^{25}$ +25 (*c* 0.1, MeOH); ECD (MeOH) nm (Δε) 201 (+3.79), 232 (−2.83); ^{1}H and ^{13}C NMR data (Table 4); HR-MS *m/z* 267.1587 $[M + H]^+$ (Calcd. for $C_{15}H_{23}O_4^+$, 267.1591).

Inulabritanoid I (**9**): colorless powder; $[\alpha]_D^{25}$ +37 (*c* 0.1, MeOH); ECD (MeOH) nm (Δε) 210 (+4.87), 220 (+1.53), 235 (−1.20); ^{1}H and ^{13}C NMR data (Table 4); HR-MS *m/z* 295.1543 $[M - H]^-$ (Calcd. for $C_{16}H_{23}O_5^-$, 295.1551).

4.4. ECD calculation

The C-5 side chain structure of compounds **2**–**7** was simplified to a methyl group due to the molecular complexity. The conformational analysis of compounds **1**–**9** was performed using the GFN-xTB method implemented in the xtb software package. Conformers with relative energy differences less than 4 kcal·mol^{-1} were selected for further refinement and harmonic vibrational frequencies at the B3LYP/6-31G(d) level, utilizing the Gaussian 09 suite [43, 44]. All optimized conformers demonstrated energy minima without imaginary frequency. The stable conformers

Table 4 ^{1}H (600 MHz) and ^{13}C NMR (150 MHz) data for compounds **8** ($CDCl_3$) and **9** (DMSO-d_6).

No.	**8**		**9**	
	δ_C	δ_H (J in Hz)	δ_C	δ_H (J in Hz)
1	41.2	1.47, m	77.1	3.14, m
		1.21, m		
2	19.0	1.63, m	27.2	1.54, m
		1.59, m		1.49, m
3	40.1	1.83, m	33.8	1.62, m
		1.81, m		1.53, m
4	72.1		74.8	
5	59.2	1.90, d (11.6)	53.1	1.90, d (11.2)
6	77.4	4.59, t (11.2)	75.9	4.39, t (11.2)
7	55.2	2.80, m	53.9	2.76, m
8	66.2	4.61, m	63.6	4.37, m
9	50.0	1.82, m	46.2	2.04, dd (14.1, 2.5)
		1.54, m		1.32, dd (14.1, 2.6)
10	38.2		42.1	
11	134.9		170.7	
12	169.5		136.1	
13	119.5	6.28, d (3.3)	117.9	5.98, d (3.2)
		5.55, d (3.3)		5.5, d (3.2)
14	22.4	1.21, s	16.3	1.07, s
15	24.5	1.41, s	19.6	1.19, s
OH-1				4.53 (4.9)
OH-8				4.81 (4.0)
OCH_3-4			47.3	3.03, s

Table 5 Inhibitory activities of compounds **1**–**27** toward LPS-induced NO release (mean ± SD, n = 3).

Compound	IC_{50}/(μmol·L^{-1})	Compound	IC_{50}/(μmol·L^{-1})
1	3.65 ± 0.15	**15**	24.77 ± 1.82
2	5.48 ± 0.35	**16**	6.91 ± 1.00
3	> 40	**17**	14.96 ± 0.43
4	> 40	**18**	25.61 ± 1.51
5	15.06 ± 0.81	**19**	3.12 ± 0.07
6	> 40	**20**	14.78 ± 0.57
7	19.58 ± 1.22	**21**	> 40
8	> 40	**22**	> 40
9	> 40	**23**	> 40
10	> 40	**24**	> 40
11	10.02 ± 1.19	**25**	> 40
12	3.29 ± 0.43	**26**	5.67 ± 0.31
13	11.14 ± 1.47	**27**	> 40
14	> 40	Indomethacin[a]	11.01 ± 0.12

[a] positive control.

were utilized for ECD calculations using B3LYP/6-311G(d), and the calculated ECD spectra were generated using SpecDis 1.64 software (Berlin, Germany) and GraphPad Prism 8.3.0 software (San Diego, CA, USA).

4.5. Cell culture and treatment

RAW264.7 cells were maintained in DMEM supplemented with 10% FBS and 1% penicillin and streptomycin, and cultured at 37 °C with 5% CO_2 [45-47]. To evaluate the anti-inflammatory effects of compounds **1**–**27**, RAW264.7 cells were seeded in 96-well plates overnight and treated with compounds prior to LPS administration (0.5 μg·mL^{-1}). After 24 h, supernatants were analyzed for NO levels following established methods [21, 48].

4.6. Enzyme-linked immunosorbent assays

TNF-α and IL-6 levels in supernatants were measured according to the manufacturer's protocol (Neobioscience, Shenzhen, China).

4.7. Real-time quantitative PCR

RNA extraction was performed using TRIzol reagent, followed by RNA concentration quantification using a NanoPhotometer NP80 system (Implen, Munich, Germany). Subsequently, complementary deoxyribonucleic acid (cDNA) synthesis was conducted using the NovoScript 1st Strand cDNA Synthesis Kit. Quantitative real-time PCR (qPCR) analysis was performed with an ABI Quant Studio 1 system (Applied Biosystems, Life Technologies, Carlsbad, USA), using SYBR Green Master Mix reagents [Accurate Biotechnology (Human) Co., Ltd., Changsha, China].

4.8. Western blot

Cells were harvested and lysed on ice for 2 h in a lysis buffer containing 1% protease inhibitors and PMSF. Equal protein amounts were separated by 10% SDS-PAGE at 80 V for 2 h, then transferred to PVDF membranes for 30–150 min. Membranes were blocked with 5% skimmed milk for 2 h and incubated overnight at 4 °C with appropriate primary antibodies specific to protein markers. After washing with TBST, membranes were incubated with secondary antibodies for 1 h at room temperature. Finally, the membranes were treated with an ECL reagent mixture and visualized using the ChemiScope 6200 Touch imaging system (Shanghai, China).

Funding

This work was supported by the National Natural Science Foundation of China (Nos. 82274069, 82030116, and 82141212), the Young Scientific and Technological Talents (Level Two) in Tianjin (No. QN20230212), Tianjin Education Commission Research Program Project (No. 2024KJ004), and the Eaglet Plan Project of Tianjin University of Traditional Chinese Medicine (No. XJS2024101).

Declaration of competing interest

These authors have no conflict of interest to declare.

References

1 Sun CP, Jia ZL, Huo XK, et al. Medicinal *Inula* species: phytochemistry, biosynthesis, and bioactivities. *Am J Chin Med*. 2021;49(2):315-358. https://doi.org/10.1142/S0192415X21500166.
2 Zhao WY, Yan JJ, Zhang M, et al. Natural soluble epoxide hydrolase inhibitors from *Inula britanica* and their potential interactions with soluble epoxide hydrolase: insight from inhibition kinetics and molecular dynamics. *Chem Biol Interact*. 2021;345:109571. https://doi.org/10.1016/j.cbi.2021.109571.
3 Yang L, Wang X, Hou A, et al. A review of the botany, traditional uses, phytochemistry, and pharmacology of the Flos Inulae. *J Ethnopharmacol*. 2021;276:114125. https://doi.org/10.1016/j.jep.2021.114125.
4 *The Pharmacopoeia of the People's Republic of China*. Beijing: The Medicine Science and echnology Press of China, 2020.
5 Hong CR, Lee EH, Jung YH, et al. Development and characterization of *Inula britannica* extract-loaded liposomes: potential as anti-inflammatory functional food ingredients. *Antioxidants (Basel)*. 2023;12(8):1636. https://doi.org/10.3390/antiox12081636.
6 Lee NK, Jeewanthi RK, Park EH, et al. Short communication: physicochemical and antioxidant properties of cheddar-type cheese fortified with *Inula britannica* extract. *J Dairy Sci*. 2016;99(1):83-88. https://doi.org/10.3168/jds.2015-9935.
7 Bae WY, Kim HY, Kim KT, et al. Inhibitory effects of *Inula britannica* extract fermented by *Lactobacillus plantarum* KCCM 11613P on coagulase activity and growth of *Staphylococcus aureus* including methicillin-resistant strains. *J Food Biochem*. 2019;43(4):e12785. https://doi.org/10.1111/jfbc.12785.
8 Zheng S, Li L, Li N, et al. 1,6-*O*,*O*-Diacetylbritannilactone from *Inula britannica* induces anti-tumor effect on oral squamous cell carcinoma *via* miR-1247-3p/LXRalpha/ABCA1 signaling. *Onco Targets Ther*. 2020;13:11097-11109. https://doi.org/10.2147/OTT.S263014.
9 Zhang C, Song YG, Sun XY, et al. Photoredox-catalyzed reaction as a powerful tool for rapid natural product gem-dimethylation modification: discovery of potent anti-cancer agents with improved druggability. *Acta Mater Med*. 2023;2:400-408. https://doi.org/10.15212/AMM-2023-0032.
10 Zhang J, Liu J, Liu JW, et al. Targeting Keap1 with Inulae Herba activated the Nrf2 receptor to alleviate LPS-mediated acute lung injury. *J Ethnopharmacol*. 2024;319(Pt 3):117358. https://doi.org/10.1016/j.jep.2023.117358.
11 Zhang J, Zhang M, Zhang WH, et al. Total flavonoids of *Inula japonica* alleviated the inflammatory response and oxidative stress in LPS-induced acute lung injury *via* inhibiting the sEH activity: insights from lipid metabolomics. *Phytomedicine*. 2022;107:154380. https://doi.org/10.1016/j.phymed.2022.154380.
12 Zhang J, Zhang M, Zhang WH, et al. Total terpenoids of *Inula japonica* activated the Nrf2 receptor to alleviate the inflammation and oxidative stress in LPS-induced acute lung injury. *Phytomedicine*. 2022;107:154377. https://doi.org/10.1016/j.phymed.2022.154377.
13 Zhang M, Zhang J, Zhu QM, et al. *Inula japonica* ameliorated the inflammation and oxidative stress in LPS-induced acute lung injury through the MAPK/NF-kappaB and Keap1/Nrf2 signalling pathways. *J Pharm Pharmacol*. 2023;75(2):287-299. https://doi.org/10.1093/jpp/rgac084.
14 Guo C, Geng HJ, Wang WJ, et al. Dimerized sesquiterpenoid [4 + 2] adducts with ferroptosis-promoting activity from *Inula britannica* Linn. *Phytochemistry*. 2024;218:113951. https://doi.org/10.1016/j.phytochem.2023.113951.
15 Tang JJ, Guo C, Peng XN, et al. Chemical characterization and multifunctional neuroprotective effects of sesquiterpenoid-enriched *Inula britannica* flowers extract. *Bioorg Chem*. 2021;116:105389. https://doi.org/10.1016/j.bioorg.2021.105389.
16 Cai YS, Wu Z, Wang JR, et al. Spiroalanfurantones A–D, four eudesmanolide-furan sesquiterpene adducts with a pentacyclic 6/6/5/5/5 skeleton from *Inula helenium*. *Org Lett*. 2019;21(23):9478-9482. https://doi.org/10.1021/acs.orglett.9b03676.
17 Jin Q, Lee JW, Jang H, et al. Dimeric- and trimeric sesquiterpenes from the flower of *Inula japonica*. *Phytochemistry*. 2018;155:107-113. https://doi.org/10.1016/j.phytochem.2018.07.008.
18 Lee IS, Lee YR, Sim JH, et al. The effects of 1-*O*-acetylbritannilactone isolated from *Inula britannica* flowers on human neutrophil elastase and inflammation of RAW 264.7 cells and *Zebrafish Larvae*. *Molecules*. 2023;28(11):4320. https://doi.org/10.3390/molecules28114320.
19 Hong JY, Kim H, Lee J, et al. Neurotherapeutic effect of *Inula britannica* var. *chinensis* against H_2O_2-induced oxidative stress and mitochondrial dysfunction in cortical neurons. *Antioxidants (Basel)*. 2021;10(3):375. https://doi.org/10.3390/antiox10030375.
20 Zhang J, Yang FY, Zhu QM, et al. Inhibition effect of 1-acetoxy-6*α*-(2-methylbutyryl)eriolanolide toward soluble epoxide hydrolase: multispectral analysis, molecular dynamics simulation, biochemical, and *in vitro* cell-based studies. *Int J Biol Macromol*. 2023;235:123911. https://doi.org/10.1016/j.ijbiomac.2023.123911.
21 Zhang J, Zhang M, Huo XK, et al. Macrophage inactivation by small molecule wedelolactone *via* targeting sEH for the treatment of LPS-induced acute lung injury. *ACS Cent Sci*. 2023;9(3):440-456. https://doi.org/10.1021/acscentsci.2c01424.
22 Zhang J, Zhang M, Zhu QM, et al. Allosteric regulation of Keap1 by 8*β*-hydroxy-*α*-cyclocostunolide for the treatment of acute lung injury. *Acta Pharm Sin B*. 2024;9:4174-4178. https://doi.org/10.1016/j.apsb.2024.06.025.
23 Jin HZ, Lee D, Lee JH, et al. New sesquiterpene dimers from *Inula britannica* inhibit NF-κB activation and NO and TNF-α production in LPS-stimulated RAW264.7 cells. *Planta Med*. 2006;72(1):40-45. https://doi.org/10.1055/s-2005-873189.
24 Wu RF, Wang WQ, Zhou BD, et al. Anti-inflammatory sesquiterpene dimers and diterpenes from the aerial part of *Inula japonica*. *J Asian Nat Prod Res*. 2022;24(4):328-335. https://doi.org/10.1080/10286020.2021.1923012.
25 Qin JJ, Jin HZ, Fu JJ, et al. Japonicones A–D, bioactive dimeric sesquiterpenes from *Inula japonica* Thunb. *Bioorg Med Chem Lett*. 2009;19(3):710-713. https://doi.org/10.1016/j.bmcl.2008.12.043.
26 Xu XY, Sun P, Guo DA, et al. Cytotoxic sesquiterpene lactone dimers isolated from *Inula japonica*. *Fitoterapia*. 2015;101:218-223. https://doi.org/10.1016/j.fitote.2015.01.011.

27 Dong S, Tang JJ, Zhang CC, et al. Semisynthesis and *in vitro* cytotoxic evaluation of new analogues of 1-*O*-acetylbritannilactone, a sesquiterpene from *Inula britannica*. *Eur J Med Chem*. 2014;80:71-82. https://doi.org/10.1016/j.ejmech.2014.04.028.

28 Qin JJ, Jin HZ, Zhu JX, et al. New sesquiterpenes from *Inula japonica* Thunb. with their inhibitory activities against LPS-induced NO production in RAW264.7 macrophages. *Tetrahedron*. 2010;66(1):9379-9388. https://doi.org/10.1016/j.tet.2010.09.091.

29 Yang C, Wang CM, Jia ZJ. Sesquiterpenes and other constituents from the aerial parts of *Inula japonica*. *Planta Med*. 2003;69(7):662-666. https://doi.org/10.1055/s-2003-41123.

30 Wu XD, Ding LF, Tu WC, et al. Bioactive sesquiterpenoids from the flowers of *Inula japonica*. *Phytochemistry*. 2016;129:68-76. https://doi.org/10.1016/j.phytochem.2016.07.008.

31 Locksley HD, Fayez MBE, Radwan AS, et al. Constituents of local plants XXV, constitution of the antispasmodic principle of *Cymbopogon proximus*. *Planta Med*. 1982;46:20-22.

32 Park EJ, Kim J. Cytotoxic sesquiterpene lactones from *Inula britannica*. *Planta Med*. 1998;64(8):752-754. https://doi.org/10.1055/s-2006-957573.

33 Cardona ML, Fernández I, García B, et al. Revision of the structure of an eudesmanolide isolated from *Lasiolaena santosii*. *J Nat Prod*. 1990;53:1042-1045. https://doi.org/10.1021/np50070a051.

34 Eiroa JL, Triana J, Pérez FJ, et al. Secondary metabolites from two Hispaniola *Ageratina* species and their cytotoxic activity. *Med Chem Res*. 2018;27:1792-1799. https://doi.org/10.1007/s00044-018-2192-y.

35 Sun CP, Zhou JJ, Yu ZL, et al. Kurarinone alleviated Parkinson's disease *via* stabilization of epoxyeicosatrienoic acids in animal model. *Proc Natl Acad Sci U S A*. 2022;119(9):e2118818119. https://doi.org/10.1073/pnas.2118818119.

36 Zhang J, Luan ZL, Huo XK, et al. Direct targeting of sEH with alisol B alleviated the apoptosis, inflammation, and oxidative stress in cisplatin-induced acute kidney injury. *Int J Biol Sci*. 2023;19(1):294-310. https://doi.org/10.7150/ijbs.78097.

37 Zhang J, Zhang WH, Morisseau C, et al. Genetic deletion or pharmacological inhibition of soluble epoxide hydrolase attenuated particulate matter 2.5 exposure mediated lung injury. *J Hazard Mater*. 2023;458:131890. https://doi.org/10.1016/j.jhazmat.2023.131890.

38 Yang L, Xu HH, Hong Q, et al. *Crocus sativus* L. produces anti-inflammatory effects and regulates NLRP3-NF-κB pathway. *Acup Herb Med*. 2024;4(3):375-385. https://doi.org/10.1097/HM9.0000000000000088.

39 Yang M, Oppong MB, Di J, et al. Steroidal saponins with anti-inflammatory activity from *Tribulus terrestris* L. *Acup Herb Med*. 2022;2:41-48. https://doi.org/10.1097/HM9.0000000000000026.

40 Zhang J, Zhang R, Li W, et al. IkappaB kinase beta (IKKβ): structure, transduction mechanism, biological function, and discovery of its inhibitors. *Int J Biol Sci*. 2023;19(13):4181-4203. https://doi.org/10.7150/ijbs.85158.

41 Mitchell S, Vargas J, Hoffmann A. Signaling *via* the NFκB system. *Wiley Interdiscip Rev Syst Biol Med*. 2016;8(3):227-241. https://doi.org/10.1002/wsbm.1331.

42 Motohashi H, Yamamoto M. Nrf2-Keap1 defines a physiologically important stress response mechanism. *Trends Mol Med*. 2004;10(11):549-557. https://doi.org/10.1016/j.molmed.2004.09.003.

43 Wang C, Huo XK, Luan ZL, et al. Alismanin A, a triterpenoid with a C_{34} skeleton from *Alisma orientale* as a natural agonist of human pregnane X receptor. *Org Lett*. 2017;19(20):5645-5648. https://doi.org/10.1021/acs.orglett.7b02738.

44 Liang JH, Luan ZL, Tian XG, et al. Uncarialins A–I, monoterpenoid indole alkaloids from *Uncaria rhynchophylla* as natural agonists of the 5-HT(1A) receptor. *J Nat Prod*. 2019;82(12):3302-3310. https://doi.org/10.1021/acs.jnatprod.9b00532.

45 Chen J, Zhang Q, Guo J, et al. Single-cell transcriptomics reveals the ameliorative effect of rosmarinic acid on diabetic nephropathy-induced kidney injury by modulating oxidative stress and inflammation. *Acta Pharm Sin B*. 2024;14(4):1661-1676. https://doi.org/10.1016/j.apsb.2024.01.003.

46 Liu H, Wang H, Li Q, et al. LPS adsorption and inflammation alleviation by polymyxin B-modified liposomes for atherosclerosis treatment. *Acta Pharm Sin B*. 2023;13(9):3817-3833. https://doi.org/10.1016/j.apsb.2023.06.005.

47 Wei W, Zeng Q, Wang Y, et al. Discovery and identification of EIF2AK2 as a direct key target of berberine for anti-inflammatory effects. *Acta Pharm Sin B*. 2023;13(5):2138-2151. https://doi.org/10.1016/j.apsb.2022.12.009.

48 Wang W, Xiong LL, Wu YL, et al. New lathyrane diterpenoid hybrids have anti-inflammatory activity through the NF-κB signaling pathway and autophagy. *Acta Mater Med*. 2022;1:224-243. https://doi.org/10.15212/AMM-2022-0008.